Original Scientific Paper

An Unconditionally Stable Spectral-Finite Difference Scheme for the Nonlinear Time-Fractional Klein-Gordon-Zakharov System

Soheila Mirzaei and Ali Shokri*

Abstract

This study presents an innovative numerical scheme to address the nonlinear time-fractional coupled Klein-Gordon-Zakharov equation. The spatial derivatives are approximated using a pseudo-spectral method, which utilizes Lagrange polynomials at Chebyshev points as basis functions. Time discretization is accomplished through the finite difference method. The proposed scheme is rigorously proven to be unconditionally stable, ensuring robustness in numerical simulations. Furthermore, the time convergence order of the scheme is derived, highlighting its reliability. Numerical experiments demonstrate the exceptional accuracy and robustness of the method, with its exponential precision offering precise and reliable solutions. This approach serves as a powerful tool for solving complex non-linear partial differential equations, making it highly applicable in various scientific and engineering domains that demand effective and efficient computational techniques.

Keywords: Coupled Klein-Gordon-Zakharov Equation, Fractional derivatives, Pseudo-spectral method, Chebyshev points, Lagrange polynomials.

2020 Mathematics Subject Classification: 65M70, 35R11.

How to cite this article

S. Mirzaei and A. Shokri, An unconditionally stable spectral-finite difference scheme for the nonlinear time-fractional Klein-Gordon-Zakharov system, Math. Interdisc. Res. 10 (4) (2025) 365-384.

*Corresponding author (E-mail: a.shokri@znu.ac.ir) Academic Editor: Akbar Mohebbi

Received 7 April 2025, Accepted 2 August 2025

DOI: 10.22052/MIR.2025.256648.1513

© 2025 University of Kashan

This work is licensed under the Creative Commons Attribution 4.0 International License.

1. Introduction

During the last few decades, fractional differential equations (FDEs) have been significantly used in several models, including signal processing, traffic flow and diffusion models, and the fluid flow model [1–4]. Also, non-integer calculus has been given attention in some fields of mathematical biology, electro-chemistry [5], and different physical phenomena, including relative stress and strain for elastic or viscoelastic materials and Hook's law [4, 6, 7].

Plasma, which consists of two intertwined fluids —the electron fluid and the ion fluid— is modeled. These fluids exhibit different behaviors on two distinct timescales: fast and slow. The significant disparity in mass between electrons and ions gives rise to this dichotomy. When subjected to an external force, electrons accelerate much more rapidly than ions due to their significantly lower mass. Specifically, we define u(x,t) as a complex function related to the fast timescale component of the electric field generated by electrons, and v(x,t) as the real function representing the deviation of ion density from its equilibrium state. To describe the interaction between Langmuir waves and ion-acoustic waves in plasma, we can use coupled Klein-Gordon-Zakharov (KGZ) equations [8–10]

$$\begin{cases} \frac{\partial^{\alpha} u}{\partial t^{\alpha}} = \Delta u - u - uv - |u|^{2} u + f, \\ \frac{\partial^{\beta} v}{\partial t^{\beta}} = \Delta v + \Delta (|u|^{2}) + g, \end{cases}$$
 (1)

where $1 \le \alpha, \beta \le 2$, and with the following initial conditions

$$\begin{cases} u(x,0) = u_0(x), \\ \frac{\partial u}{\partial t}(x,0) = u_1(x), \end{cases} \begin{cases} v(x,0) = v_0(x), \\ \frac{\partial v}{\partial t}(x,0) = v_1(x), \end{cases}$$
(2)

for $x \in \Omega \subseteq \mathbb{R}^2$, and the homogeneous boundary conditions

$$u(x,t) = 0,$$
 $v(x,t) = 0,$ $x \in \partial\Omega, t \in [0,T].$ (3)

Here f, g, u_0, u_1, v_0 , and v_1 are known smooth functions, Ω is a rectangle in \mathbb{R}^2 , and T > 0 is the final time. The $\frac{\partial^{\alpha} u}{\partial t^{\alpha}}$ and $\frac{\partial^{\beta} v}{\partial t^{\beta}}$ denote the Caputo-type fractional derivative of order α and β , respectively.

The Caputo fractional derivative of order α is defined as

$$^{C}D_{x}^{\alpha}f(x) = \frac{1}{\Gamma(n-\alpha)}\int_{0}^{x} \frac{f^{(n)}(t)}{(x-t)^{\alpha+1-n}}dt, \quad n-1 < \alpha < n,$$

where $\Gamma(\cdot)$ is the Gamma function [4, 6].

The KGZ equations exhibit a shape similar to both the Zakharov equations and the Klein-Gordon-Schrödinger equations. Researchers have investigated the existence of solutions and the stability behavior of KGZ equations in various studies, as referenced by the following works: [11–14].

Ray and Sahoo [15] employed the homotopy disorder transformation method and the modified homotopy analysis method to derive approximate solutions for the KGZ equation. In another study [16], the trivial conservation laws and exact solutions were further modified and extended using the hyperbolic function method for the non-linear coupled KGZ equation. Jia et al. [17] utilized an efficient exponential sum approximation to estimate time dependencies while employing the Fourier spectral method to approximate spatial derivatives in the KGZ equation. Additionally, several other numerical methods have been implemented for solving KGZ equations, including the q-homotopy analysis transform method (q-HATM) [18], the quintic B-spline based differential quadrature method [19], and the Differential Quadrature (DQ) and Globally Radial Basis Functions (GRBFs) methods [9].

This paper comprises six sections. In the second section, we explain the method of discretizing the time derivatives. In the third section, we introduce the pseudo-spectral method and apply it to the non-linear coupled KGZ equation, resulting in the final discretized equation. In the subsequent section, we demonstrate that the presented scheme is unconditionally stable. Moving on to the fifth section, we showcase the effectiveness of the proposed method by implementing three test problems. Finally, we give the conclusion of this paper.

2. Time discretization scheme

In this section, we discuss how to discretize the time derivative terms. Considering that the time derivation is fractional, we introduce some definitions and lemmas to do this.

Let $u^k = u(x, t_k)$ is a grid function on $\Omega \times (0, T)$. We introduce the following symbols:

$$u^{k-1/2} = \frac{1}{2} \left(u^k + u^{k-1} \right), \qquad \delta_t u^{k-1/2} = \frac{1}{\eta} \left(u^k - u^{k-1} \right),$$

$$\delta_x^2 u^{k-1/2} = \frac{1}{2} \left(\delta_x^2 u^k + \delta_x^2 u^{k-1} \right), \tag{4}$$

where $t_k = k\eta$ $(k = 0, 1, \dots, N)$, and η is the time step size.

The approximations of the fractional time derivatives in Equation (1) are given as [20]

$$\frac{\partial^{\alpha} u^{k}}{\partial t^{\alpha}} \approx \frac{1}{\eta \Gamma(2-\alpha)} \left[\mu_{0} \delta_{t} u^{k-1/2} - \sum_{i=1}^{k-1} (\mu_{k-i-1} - \mu_{k-i}) \, \delta_{t} u^{i-1/2} - \mu_{k-1} \phi_{1} \right], \quad (5)$$

$$\frac{\partial^{\beta} v^{k}}{\partial t^{\beta}} \approx \frac{1}{\eta \Gamma(2-\beta)} \left[\hat{\mu}_{0} \delta_{t} v^{k-1/2} - \sum_{i=1}^{k-1} \left(\hat{\mu}_{k-i-1} - \hat{\mu}_{k-i} \right) \delta_{t} v^{i-1/2} - \hat{\mu}_{k-1} \phi_{2} \right], \quad (6)$$

where $\phi_1 = \frac{\partial u}{\partial t}|_{t=0}$ and $\phi_2 = \frac{\partial v}{\partial t}|_{t=0}$. The coefficients μ_j and $\hat{\mu}_j$ are obtained as

$$\mu_j = \int_{t_i}^{t_{j+1}} \frac{dt}{t^{\alpha - 1}} = \frac{\eta^{2 - \alpha}}{2 - \alpha} \left[(j+1)^{2 - \alpha} - (j)^{2 - \alpha} \right], \quad j \ge 0, \tag{7}$$

$$\hat{\mu}_j = \int_{t_j}^{t_{j+1}} \frac{dt}{t^{\beta - 1}} = \frac{\eta^{2 - \beta}}{2 - \beta} \left[(j + 1)^{2 - \beta} - (j)^{2 - \beta} \right], \quad j \ge 0.$$
 (8)

Lemma 2.1. ([20]). Let $h(t) \in C^2[0, t_k]$, then we have

$$\left| \int_0^{t_k} h'(t) \frac{dt}{(t_k - t)^{\alpha - 1}} - \frac{1}{\eta} \left[\mu_0 h(t_k) - \sum_{j=1}^{k-1} (\mu_{k-j-1} - \mu_{k-j}) h(t_j) - \mu_{k-1} h(t_0) \right] \right|$$

$$\leq \frac{1}{2 - \alpha} \left[\frac{2 - \alpha}{12} + \frac{2^{3 - \alpha}}{3 - \alpha} - (1 + 2^{1 - \alpha}) \right] \max_{1 \leq t \leq t_k} |h''(t)| \eta^{3 - \alpha},$$

where μ_i is defined in (7) and $1 < \alpha < 2$.

Therefore, according to the Lemma 2.1, the accuracy of approximations (5) and (6) are of orders $\eta^{3-\alpha}$ and $\eta^{3-\beta}$, respectively. Now, using the approximations (4)-(6), we obtain the time discrete scheme of coupled KGZ equation (1) as

$$\frac{1}{\eta\Gamma(2-\alpha)} \left[\mu_0 \delta_t u^{k-1/2} - \sum_{i=1}^{k-1} (\mu_{k-i-1} - \mu_{k-i}) \, \delta_t u^{i-1/2} - \mu_{k-1} \phi_1 \right] = \delta_x^2 u^{k-1/2}
+ \delta_y^2 u^{k-1/2} - u^{k-1/2} - (uv)^{k-1/2} - (|u|^2 u)^{k-1/2} + f^{k-1/2}, \qquad (9)$$

$$\frac{1}{\eta\Gamma(2-\beta)} \left[\hat{\mu}_0 \delta_t v^{k-1/2} - \sum_{i=1}^{k-1} (\hat{\mu}_{k-i-1} - \hat{\mu}_{k-i}) \, \delta_t v^{i-1/2} - \hat{\mu}_{k-1} \phi_2 \right] = \delta_x^2 v^{k-1/2}
+ \delta_y^2 v^{k-1/2} + \Delta(|u|^2)^{k-1/2} + g^{k-1/2}, \qquad (10)$$

for k = 1, 2, ..., N. In the next section, we will discuss how to apply the pseudo-spectral method on the Equations (9)-(10).

3. The Pseudo-spectral method

In this section, we give a brief explanation of the pseudo-spectral methods (for more information about the spectral and pseudo-spectral methods, see [21]). In pseudo-spectral methods, choosing the bases of the approximation space is very important. In this work, we present a suitable approximation of the solution in terms of Lagrange polynomials, which leads to spectral accuracy or exponential convergence. Note that we use the pseudo-spectral method only to discretize the spatial variable. Also, we describe the implementation of the method for the two-dimensional case.

Suppose $\Omega \subseteq \mathbb{R}^2$ is a bounded rectangle domain and n_p is a positive integer. We consider Chebyshev points as nodal points

$$x_{ij} = (\cos(i\pi/n_p), \cos(j\pi/n_p)), \quad i, j = 0, 1, \dots, n_p.$$
 (11)

We consider the solutions of the KGZ equation (1) as a linear combination of Lagrange polynomials as

$$u(x,t) = \sum_{i,j=1}^{n_p-1} u_{ij}(t)\ell_{ij}(x), \quad u_{ij}(t) := u(x_{ij},t),$$
(12)

$$v(x,t) = \sum_{i,j=1}^{n_p-1} v_{ij}(t)\ell_{ij}(x), \quad v_{ij}(t) := v(x_{ij},t),$$
(13)

where ℓ_{ij} are Lagrange polynomials, which are defined as

$$\ell_{ij}(x,y) = \ell_i(x)\ell_j(y), \quad i, j = 0, 1, \dots, n_p,$$

$$\ell_i(x) = \prod_{\substack{k=0\\k \neq i}}^{n_p} \left(\frac{x - x_k}{x_i - x_k} \right), \quad i = 0, 1, \dots, n_p.$$

Note that $\ell_i(x) \in \mathbb{P}_{n_p}$ (polynomials of degree $\leq n_p$) and satisfy in the Kronecker Delta property

$$\ell_i(x_j) = \delta_{ij}, \quad i, j = 0, 1, \cdots, n_p.$$

We could find the second-order derivatives of $\ell_{ij}(\cdot)$ concerning x and y in Chebyshev nodal points (11) as

$$\frac{\partial^2}{\partial x^2} \ell_{ij}(x_{rs}) = \ell_i''(x_r) \ell_j(y_s) = \left[D_{n_p}^2 \right]_{ri} \delta_{js},$$

$$\frac{\partial^2}{\partial y^2} \ell_{ij}(x_{rs}) = \ell_i(x_r) \ell_j''(y_s) = \delta_{ri} \left[D_{n_p}^2 \right]_{is},$$

where $r, s = 0, 1, \dots, n_p$. Applying relations (12)-(13) and (5)-(6) to the Equation (1), we have

$$\nu_{1}\mu_{0}u_{rs}^{m} - \frac{1}{2} \sum_{i,j=1}^{n_{p}-1} \Delta \ell_{ij}(x_{rs})u_{ij}^{m} + \frac{1}{2}u_{rs}^{m} = \nu_{1}\mu_{0}u_{rs}^{m-1}$$

$$+ \frac{1}{2} \sum_{i,j=1}^{n_{p}-1} \Delta \ell_{ij}(x_{rs})u_{ij}^{m-1} - \frac{1}{2}u_{rs}^{m-1} - u_{rs}^{m-1}v_{rs}^{m-1} - (|u_{rs}|^{2})^{m-1}u_{rs}^{m-1}$$

$$+ \nu_{1} \sum_{i=1}^{m-1} (\mu_{m-i-1} - \mu_{m-i}) \delta_{t}u_{rs}^{i-1/2} + \nu_{1}\mu_{m-1}\phi_{1}$$

$$+ f_{rs}^{m-1}, \quad r, s = 0, 1, \cdots, n_{p},$$

$$\nu_{2}\hat{\mu}_{0}v_{rs}^{m} - \frac{1}{2} \sum_{i,j=1}^{n_{p}-1} \Delta \ell_{ij}(x_{rs})v_{ij}^{m} = \nu_{2}\hat{\mu}_{0}v_{rs}^{m-1} + \frac{1}{2} \sum_{i,j=1}^{n_{p}-1} \Delta \ell_{ij}(x_{rs})v_{ij}^{m-1}$$

$$+ \sum_{i,j=1}^{n_{p}-1} \Delta \ell_{ij}(x_{rs})(|u_{ij}|^{2})^{m-1} + \nu_{2} \sum_{i=1}^{m-1} (\hat{\mu}_{m-i-1} - \hat{\mu}_{m-i}) \delta_{t}v_{rs}^{i-1/2}$$

$$+ \nu_{2}\hat{\mu}_{m-1}\phi_{2} + g_{rs}^{m-1}, \quad r, s = 0, 1, \cdots, n_{p}.$$

$$(14)$$

where $f_{rs}^m=f(x_{rs},t^m),\,g_{rs}^m=g(x_{rs},t^m),\,\nu_1=\frac{1}{\eta^2\Gamma(2-\alpha)}$ and $\nu_2=\frac{1}{\eta^2\Gamma(2-\beta)}$ are two constant coefficients, and $\eta=T/N$ is the time step. In addition,

$$\Delta \ell_{ij}(x_{rs}) = \left[D_{n_p}^2 \right]_{ri} \delta_{js} + \delta_{ri} \left[D_{n_p}^2 \right]_{js}, \quad r, s = 0, 1, \dots, n_p,$$
 (16)

where $D_{n_p}^2$ is the second-order derivative matrix in Chebyshev points [22].

4. Stability

In this section, we present a theorem along with its proof to demonstrate that the method described in Section 2 exhibits unconditional stability. To facilitate the stability analysis, we introduce the following operators:

$$\mathcal{P}\left(u^{n-\frac{1}{2}},\phi_1\right) = \mu_0 u^{n-1/2} - \sum_{k=1}^{n-1} \left(\mu_{n-k-1} - \mu_{n-k}\right) u^{k-1/2} - \mu_{n-1}\phi_1,\tag{17}$$

$$\hat{\mathcal{P}}\left(v^{n-\frac{1}{2}},\phi_2\right) = \hat{\mu}_0 v^{n-1/2} - \sum_{k=1}^{n-1} \left(\hat{\mu}_{n-k-1} - \hat{\mu}_{n-k}\right) v^{k-1/2} - \hat{\mu}_{n-1}\phi_2. \tag{18}$$

Using these operators, we can write the time discrete schemes (9)-(10) as

$$\begin{cases}
\frac{1}{\eta\Gamma(2-\alpha)}\mathcal{P}\left(\delta_{t}u^{n-\frac{1}{2}},\phi_{1}\right) = \Delta u^{n-\frac{1}{2}} - u^{n-\frac{1}{2}} - (uv)^{n-\frac{1}{2}} - (|u|^{2}u)^{n-\frac{1}{2}} + f^{n-\frac{1}{2}}, \\
\frac{1}{\eta\Gamma(2-\beta)}\hat{\mathcal{P}}\left(\delta_{t}v^{n-\frac{1}{2}},\phi_{2}\right) = \Delta v^{n-\frac{1}{2}} + \Delta(|u|^{2})^{n-\frac{1}{2}} + g^{n-\frac{1}{2}}, \\
u^{n} = v^{n} = 0, \quad x \in \partial\Omega,
\end{cases}$$
(19)

By using Lemma:

Lemma 4.1. ([23]). For any $\Phi = {\Phi_1, \Phi_2, \cdots}$ and ϕ , we obtain

$$\sum_{n=1}^{N} \mathcal{P}\left(\Phi_{n}, \phi\right) \Phi_{n} \geq \frac{t_{N}^{1-\alpha}}{2} \eta \sum_{n=1}^{N} \Phi_{n}^{2} - \frac{t_{N}^{2-\alpha}}{2(2-\alpha)} \phi^{2}, \qquad \forall N = 1, 2, \dots.$$

we have the following theorem for the stability of the scheme.

Theorem 4.2. Asumme $u^n, v^n \in H_0^1(\Omega)$ and $\phi_1 = \frac{\partial u}{\partial t}|_{t=0}, \phi_2 = \frac{\partial v}{\partial t}|_{t=0}$. Then the time discrete scheme (19) are unconditionally stable and we have the following inequality

$$||u^n||_{L^2(\Omega)} \le C_1, \qquad ||v^n||_{L^2(\Omega)} \le C_2,$$

where C_1, C_2 are positive constant.

Proof. By multiplying the two sides of the equations in (19) by $\delta_t u^{n-\frac{1}{2}}$ and $\delta_t v^{n-\frac{1}{2}}$ respectively, and taking the integral over the Ω , we have

$$\frac{1}{\eta\Gamma(2-\alpha)} \left\{ \mu_0(\delta_t u^{n-\frac{1}{2}}, \delta_t u^{n-\frac{1}{2}}) - \sum_{k=1}^{n-1} (\mu_{n-k-1} - \mu_{n-k}) (\delta_t u^{k-\frac{1}{2}}, \delta_t u^{n-\frac{1}{2}}) - \mu_{n-1}(\phi_1, \delta_t u^{n-\frac{1}{2}}) \right\} \\
= (\nabla^2 u^{n-\frac{1}{2}}, \delta_t u^{n-\frac{1}{2}}) - ((u^{n-\frac{1}{2}}), \delta_t u^{n-\frac{1}{2}}) - ((uv)^{n-\frac{1}{2}}, \delta_t u^{n-\frac{1}{2}}) \\
- ((|u|^2 u)^{n-\frac{1}{2}}, \delta_t u^{n-\frac{1}{2}}) + (f^{n-\frac{1}{2}}, \delta_t u^{n-\frac{1}{2}}), \tag{20}$$

$$\frac{1}{\eta\Gamma(2-\beta)} \left\{ \hat{\mu}_0(\delta_t v^{n-\frac{1}{2}}, \delta_t v^{n-\frac{1}{2}}) - \sum_{k=1}^{n-1} (\hat{\mu}_{n-k-1} - \hat{\mu}_{n-k}) (\delta_t v^{k-\frac{1}{2}} \delta_t v^{n-\frac{1}{2}}) - \hat{\mu}_{n-1}(\phi_2, \delta_t v^{n-\frac{1}{2}}) \right\} \\
= (\nabla^2 v^{n-\frac{1}{2}}, \delta_t v^{n-\frac{1}{2}}) + (\nabla^2 (|u|^2)^{n-\frac{1}{2}}, \delta_t v^{n-\frac{1}{2}}) + (g^{n-\frac{1}{2}}, \delta_t v^{n-\frac{1}{2}}). \tag{21}$$

Using the $L^2(\Omega)$ -norm we obtain

$$\frac{1}{\eta\Gamma(2-\alpha)} \left\{ \mu_0 \|\delta_t u^{n-\frac{1}{2}}\|_{L^2(\Omega)}^2 - \sum_{k=1}^{n-1} (\mu_{n-k-1} - \mu_{n-k}) \|\delta_t u^{k-\frac{1}{2}}\|_{L^2(\Omega)} \|\delta_t u^{n-\frac{1}{2}}\|_{L^2(\Omega)} \right. \\
\left. - \mu_{n-1} \|\phi_1\|_{L^2(\Omega)} \|\delta_t u^{n-\frac{1}{2}}\|_{L^2(\Omega)} \right\} \le -(\nabla u^{n-\frac{1}{2}}, \nabla \delta_t u^{n-\frac{1}{2}}) - (u^{n-\frac{1}{2}}, \delta_t u^{n-\frac{1}{2}}) \\
- ((uv)^{n-\frac{1}{2}}, \delta_t u^{n-\frac{1}{2}}) - ((|u|^2 u)^{n-\frac{1}{2}}, \delta_t u^{n-\frac{1}{2}}) + (f^{n-\frac{1}{2}}, \delta_t u^{n-\frac{1}{2}}), \quad (22)$$

$$\frac{1}{\eta\Gamma(2-\beta)} \left\{ \hat{\mu}_0 \|\delta_t v^{n-\frac{1}{2}}\|_{L^2(\Omega)}^2 - \sum_{k=1}^{n-1} (\hat{\mu}_{n-k-1} - \hat{\mu}_{n-k}) \|\delta_t v^{k-\frac{1}{2}}\|_{L^2(\Omega)} \|\delta_t v^{n-\frac{1}{2}}\|_{L^2(\Omega)} \right. \\
\left. - \hat{\mu}_{n-1} \|\phi_2\|_{L^2(\Omega)} \|\delta_t v^{n-\frac{1}{2}}\|_{L^2(\Omega)} \right\} \le -(\nabla v^{n-\frac{1}{2}}, \nabla \delta_t v^{n-\frac{1}{2}}) \\
+ (\nabla^2 (|u|^2)^{n-\frac{1}{2}}, \delta_t v^{n-\frac{1}{2}}) + (g^{n-\frac{1}{2}}, \delta_t v^{n-\frac{1}{2}}). \quad (23)$$

Now by considering relations

$$(u^{n-\frac{1}{2}}, \delta_t u^{n-\frac{1}{2}}) = \int_{\Omega} u^{n-\frac{1}{2}} \delta_t u^{n-\frac{1}{2}} d\Omega = \int_{\Omega} (\frac{u^n + u^{n-1}}{2}) (\frac{u^n - u^{n-1}}{\eta}) d\Omega$$

$$= \frac{1}{2\eta} \int_{\Omega} ((u^n)^2 - (u^{n-1})^2) d\Omega = \frac{1}{2\eta} \Big[\|u^n\|_{L^2(\Omega)}^2 - \|u^{n-1}\|_{L^2(\Omega)}^2 \Big],$$

$$(\nabla u^{n-\frac{1}{2}}, \nabla \delta_t u^{n-\frac{1}{2}}) = \int_{\Omega} \nabla u^{n-\frac{1}{2}} \nabla \delta_t u^{n-\frac{1}{2}} d\Omega$$

$$(24)$$

$$\begin{split} &= \int_{\Omega} (\frac{\nabla u^n + \nabla u^{n-1}}{2}) (\frac{\nabla u^n - \nabla u^{n-1}}{\eta}) d\Omega \\ &= \frac{1}{2\eta} \int_{\Omega} \left((\nabla u^n)^2 - (\nabla u^{n-1})^2 \right) d\Omega = \frac{1}{2\eta} \Big[\|\nabla u^n\|_{L^2(\Omega)}^2 - \|\nabla u^{n-1}\|_{L^2(\Omega)}^2 \Big] (25) \end{split}$$

and taking sum for $n=1,\ldots,m,$ we get the following inequalities

$$\frac{1}{\eta\Gamma(2-\alpha)} \sum_{n=1}^{m} \left\{ \mu_{0} \| \delta_{t} u^{n-\frac{1}{2}} \|_{L^{2}(\Omega)}^{2} - \sum_{k=1}^{n-1} (\mu_{n-k-1} - \mu_{n-k}) \| \delta_{t} u^{k-\frac{1}{2}} \|_{L^{2}(\Omega)} \| \delta_{t} u^{n-\frac{1}{2}} \|_{L^{2}(\Omega)} \right. \\
\left. - \mu_{n-1} \| \phi_{1} \|_{L^{2}(\Omega)} \| \delta_{t} u^{n-\frac{1}{2}} \|_{L^{2}(\Omega)} \right\} + \frac{1}{2\eta} \left[\| u^{m} \|_{L^{2}(\Omega)}^{2} - \| u^{0} \|_{L^{2}(\Omega)}^{2} \right] \\
+ \frac{1}{2\eta} \left[\| \nabla u^{m} \|_{L^{2}(\Omega)}^{2} - \| \nabla u^{0} \|_{L^{2}(\Omega)}^{2} \right] \\
\leq - \sum_{n=1}^{m} \left\{ ((uv)^{n-\frac{1}{2}}, \delta_{t} u^{n-\frac{1}{2}}) + ((|u|^{2}u)^{n-\frac{1}{2}}, \delta_{t} u^{n-\frac{1}{2}}) - (f^{n-\frac{1}{2}}, \delta_{t} u^{n-\frac{1}{2}}) \right\}, \tag{26}$$

$$\frac{1}{\eta\Gamma(2-\beta)} \sum_{n=1}^{m} \left\{ \hat{\mu}_{0} \| \delta_{t} v^{n-\frac{1}{2}} \|_{L^{2}(\Omega)}^{2} - \sum_{k=1}^{n-1} (\hat{\mu}_{n-k-1} - \hat{\mu}_{n-k}) \| \delta_{t} v^{k-\frac{1}{2}} \|_{L^{2}(\Omega)} \| \delta_{t} v^{n-\frac{1}{2}} \|_{L^{2}(\Omega)} \\
- \hat{\mu}_{n-1} \| \phi_{2} \|_{L^{2}(\Omega)} \| \delta_{t} v^{n-\frac{1}{2}} \|_{L^{2}(\Omega)} \right\} + \frac{1}{2\eta} \left[\| \nabla v^{m} \|_{L^{2}(\Omega)}^{2} - \| \nabla v^{0} \|_{L^{2}(\Omega)}^{2} \right] \\
\leq \sum_{n=1}^{\infty} \left\{ (\nabla^{2} (|u^{2}|)^{n-\frac{1}{2}}, \delta_{t} v^{n-\frac{1}{2}}) + (g^{n-\frac{1}{2}}, \delta_{t} v^{n-\frac{1}{2}}) \right\}. \tag{27}$$

Using Lemma 4.1, and the inequality

$$pq \le \frac{1}{2\theta^2} p^2 + \frac{\theta^2}{2} q^2, \qquad \forall \theta \ne 0, \tag{28}$$

we obtain

$$\frac{t_{m}^{1-\alpha}}{2\Gamma(2-\alpha)} \sum_{n=1}^{m} \|\delta_{t}u^{n-\frac{1}{2}}\|_{L^{2}(\Omega)}^{2} - \frac{t_{m}^{2-\alpha}}{2(2-\alpha)\Gamma(2-\alpha)} \|\phi_{1}\|_{L^{2}(\Omega)}^{2} \\
+ \frac{1}{2\eta} \Big[\|u^{m}\|_{L^{2}(\Omega)}^{2} - \|u^{0}\|_{L^{2}(\Omega)}^{2} \Big] \\
+ \frac{1}{2\eta} \Big[\|\nabla u^{m}\|_{L^{2}(\Omega)}^{2} - \|\nabla u^{0}\|_{L^{2}(\Omega)}^{2} \Big] \\
\leq \sum_{n=1}^{m} \Big\{ |((uv)^{n-\frac{1}{2}}, \delta_{t}u^{n-\frac{1}{2}})| + |((|u|^{2}u)^{n-\frac{1}{2}}, \delta_{t}u^{n-\frac{1}{2}})| + |(f^{n-\frac{1}{2}}, \delta_{t}u^{n-\frac{1}{2}})| \Big\}, \tag{29}$$

$$+ \frac{1}{2\eta} \Big[\|\nabla v^m\|_{L^2(\Omega)}^2 - \|\nabla v^0\|_{L^2(\Omega)}^2 \Big]$$

$$\leq \sum_{n=1}^m \Big\{ (\nabla^2 (|u^2|)^{n-\frac{1}{2}}, \delta_t v^{n-\frac{1}{2}}) + (g^{n-\frac{1}{2}}, \delta_t v^{n-\frac{1}{2}}) \Big\}.$$
(30)

Now by changing upper index of sigmas from m to n, and considering $\phi_1, \phi_2 = 0$ we have

$$||u^{n}||_{L^{2}(\Omega)}^{2} - ||u^{0}||_{L^{2}(\Omega)}^{2} + ||\nabla u^{n}||_{L^{2}(\Omega)}^{2} + ||\nabla u^{0}||_{L^{2}(\Omega)}^{2}$$

$$\leq \frac{12\eta\Gamma(2-\alpha)}{t_{n}^{1-\alpha}} \sum_{j=1}^{n} \left\{ ||((uv)^{j-\frac{1}{2}})||_{L^{2}(\Omega)}^{2} + ||((|u|^{2}u)^{j-\frac{1}{2}})||_{L^{2}(\Omega)}^{2} + ||f^{j-\frac{1}{2}}||_{L^{2}(\Omega)}^{2} \right\},$$
(31)

$$\|\nabla v^n\|_{L^2(\Omega)}^2 + \|\nabla v^0\|_{L^2(\Omega)}^2 \le \frac{8\eta\Gamma(2-\beta)}{t_n^{1-\beta}} \sum_{j=1}^n \left\{ \|(\nabla^2(|u|^2)^{j-\frac{1}{2}})\|_{L^2(\Omega)}^2 + \|g^{j-\frac{1}{2}}\|_{L^2(\Omega)}^2 \right\}. \tag{32}$$

Using the Poincare inequality

$$||u^n||_{L^2(\Omega)}^2 \le C_{\Omega} ||\nabla u^n||_{L^2(\Omega)}^2$$

$$||v^n||_{L^2(\Omega)}^2 \le \hat{C}_{\Omega} ||\nabla v^n||_{L^2(\Omega)}^2$$

we can rewrite the Equations (31)-(32) as

$$(1+C_{\Omega})\|u^{n}\|_{L^{2}(\Omega)}^{2} \leq C_{\Omega} \left(\|u^{0}\|_{L^{2}(\Omega)}^{2} + \|\nabla u^{0}\|_{L^{2}(\Omega)}^{2} + \frac{12\eta\Gamma(2-\alpha)}{t_{n}^{1-\alpha}} \sum_{j=1}^{n} \left\{ \|((uv)^{j-\frac{1}{2}})\|_{L^{2}(\Omega)}^{2} + \|((|u|^{2}u)^{j-\frac{1}{2}})\|_{L^{2}(\Omega)}^{2} + \|f^{j-\frac{1}{2}}\|_{L^{2}(\Omega)}^{2} \right\} \right),$$

$$(33)$$

$$||v^{n}||_{L^{2}(\Omega)}^{2} \leq \hat{C}_{\Omega} \left(||\nabla v^{0}||_{L^{2}(\Omega)}^{2} + \frac{8\eta\Gamma(2-\beta)}{t_{n}^{1-\beta}} \sum_{j=1}^{n} \left\{ ||(\nabla^{2}(|u|^{2})^{j-\frac{1}{2}})||_{L^{2}(\Omega)}^{2} + ||g^{j-\frac{1}{2}}||_{L^{2}(\Omega)}^{2} \right\} \right).$$

$$(34)$$

By taking the maximum from the both sides of the equations, we get

$$||u^{n}||_{L^{2}(\Omega)}^{2} \leq ||u^{0}||_{L^{2}(\Omega)}^{2} + ||\nabla u^{0}||_{L^{2}(\Omega)}^{2} + \frac{12n\eta\Gamma(2-\alpha)}{t_{n}^{1-\alpha}} \max_{1\leq j\leq n} \left\{ ||((uv)^{j-\frac{1}{2}})||_{L^{2}(\Omega)}^{2} + ||((|u|^{2}u)^{j-\frac{1}{2}})||_{L^{2}(\Omega)}^{2}, + ||f^{j-\frac{1}{2}}||_{L^{2}(\Omega)}^{2} \right\},$$

$$(35)$$

$$||v^{n}||_{L^{2}(\Omega)}^{2} \leq \hat{C}_{\Omega} \left(||\nabla v^{0}||_{L^{2}(\Omega)}^{2} + \frac{8n\eta\Gamma(2-\beta)}{t_{n}^{1-\beta}} \max_{1 \leq j \leq n} \left\{ ||(\nabla^{2}(|u|^{2})^{j-\frac{1}{2}})||_{L^{2}(\Omega)}^{2} + ||g^{j-\frac{1}{2}}||_{L^{2}(\Omega)}^{2} \right\} \right).$$

$$(36)$$

Now, by simplifying we have

$$\begin{split} \|u^n\|_{L^2(\Omega)} &\leq \|u^0\|_{L^2(\Omega)} + \|\nabla u^0\|_{L^2(\Omega)}^2 \\ &+ M \max_{1 \leq j \leq n} \Big\{ \|((uv)^{j-\frac{1}{2}})\|_{L^2(\Omega)} + \|((|u|^2u)^{j-\frac{1}{2}})\|_{L^2(\Omega)} + \|f^{j-\frac{1}{2}}\|_{L^2(\Omega)} \Big\}, \\ \|v^n\|_{L^2(\Omega)} &\leq \hat{C}_{\Omega} \|\nabla v^0\|_{L^2(\Omega)}^2 + K \max_{1 \leq j \leq n} \Big\{ \|(\nabla^2(|u|^2)^{j-\frac{1}{2}})\|_{L^2(\Omega)} + \|g^{j-\frac{1}{2}}\|_{L^2(\Omega)} \Big\}, \end{split}$$

where

$$M = \left(\frac{12 \ T \ \Gamma(2-\alpha)}{t_n^{1-\alpha}}\right)^{1/2}, \quad K = \left(\hat{C}_{\Omega} \frac{8 \ T \ \Gamma(2-\beta)}{t_n^{1-\beta}}\right)^{1/2}.$$

where $T=n\eta$ denotes the final time, which is a constant. This completes the proof.

5. Numerical outcomes

Numerical investigations are provided in this section to validate and assess the performance of the method outlined in the preceding sections. The method has been applied to three distinct test problems across two spatial dimensions. A detailed examination of the results obtained for each example is presented. Notably, all algorithms have been implemented using MATLAB software.

To assess the precision of the numerical outcomes, we employ L_2 and L_{∞} error norms. Additionally, for reporting the numerical convergence rate, we utilize the following formula:

$$\mathrm{c-order} = \frac{\log(\frac{e(i-1)}{e(i)})}{\log 2},$$

where e(i) represents the corresponding error of the numerical result for $\eta(i)$.

Test problem 1

Consider the nonlinear coupled KGZ equation (1) on $\Omega = [0, 1]^2$ with exact solutions

$$u(x, y, t) = t^2 \sin(\pi x) \sin(\pi y), \quad v(x, y, t) = t^2 \sin(2\pi x) \sin(2\pi y).$$
 (37)

Therefore, the right-hand side functions f and g can be obtained from these solutions as

$$f(x,y,t) = \left(\frac{\Gamma(3)t^{2-\alpha}}{\Gamma(3-\alpha)} + 2\pi^2t^2 + t^2 + t^4\sin(2\pi x)\sin(2\pi y)\right)\sin(\pi x)\sin(\pi y),$$

		$\alpha =$	$= 1.8, \ \beta = 1.2$	2	$\alpha =$			
n_p	η	L_{∞} -error	L_2 error	c-order	L_{∞} error	L_2 error	c-order	CPU-Time
2	1/8	1.58e - 01	1.58e - 01	_	1.67e - 01	1.67e - 01	_	0.04
4	1/64	2.00e - 03	2.36e - 03	6.30	2.20e - 03	2.61e - 03	6.25	0.06
6	1/216	2.54e - 04	4.93e - 04	2.98	1.60e - 04	3.08e - 04	3.78	0.40
8	1/512	9.78e - 05	2.39e - 04	1.38	6.44e - 05	1.53e - 04	1.31	2.83
10	1/1000	4.71e - 05	1.43e - 04	1.05	3.27e - 05	9.73e - 05	0.98	10.0
12	1/1728	2.61e - 05	9.50e - 05	0.85	1.89e - 05	6.75e - 05	0.79	67.2
14	1/2744	1.59e - 05	6.73e - 05	0.72	1.19e - 05	4.96e - 05	0.67	241.4

Table 1: The L_{∞} and L_2 errors and c-orders for u at T=1 (Test problem 1).

Table 2: The L_{∞} and L_2 errors and c-orders for v at T=1 (Test problem 1).

		$\alpha = 1.8, \ \beta = 1.2$				$\alpha =$			
n_p	η	L_{∞} -error	L_2 error	c-order		L_{∞} error	L_2 error	c-order	CPU-Time
2	1/8	1.07e + 00	1.07e + 00	_		8.88e - 01	8.88e - 01	_	0.04
4	1/64	1.36e - 01	2.68e - 01	2.97		1.18e - 01	2.56e - 01	2.92	0.06
6	1/216	1.10e - 02	1.84e - 02	3.63		1.01e - 02	1.76e - 02	3.54	0.40
8	1/512	3.64e - 03	6.95e - 03	1.59		3.32e - 03	6.21e - 03	1.61	2.83
10	1/1000	1.83e - 03	4.40e - 03	0.99		1.67e - 03	3.95e - 03	0.99	10.0
12	1/1728	1.05e - 03	3.05e - 03	0.80		9.66e - 04	2.74e - 03	0.79	67.2
_14	1/2744	6.63e - 04	2.24e - 03	0.67		6.09e - 04	2.02e - 03	0.67	241.4

$$g(x,y,t) = \left(\frac{\Gamma(3)t^{2-\beta}}{\Gamma(3-\beta)} + 4\pi^2 t^2\right) \sin(2\pi x) \sin(2\pi y) - 2\pi^2 t^4 \sin^2(\pi y) \left(\cos^2(\pi x) - \sin^2(\pi x)\right) - 2\pi^2 t^4 \sin^2(\pi x) \left(\cos^2(\pi y) - \sin^2(\pi y)\right).$$

In Tables 1 and 2, the L_{∞} and L_2 errors, along with the order of numerical convergence, are reported for u and v at T=1 in two states ($\alpha=1.8$, $\beta=1.2$, and $\alpha=1.5$, $\beta=1.6$). Additionally, the times used to run the relevant programs are given in the last column of these tables. As can be seen, the accuracy of the results improves as n_p increases and η decreases simultaneously. It should be mentioned that very good results have been obtained with relatively small n_p . Table 3 reports the L_{∞} and L_2 errors along with the order of convergence for a fixed time step. Table 4 presents the same values for a fixed n_p across varying time steps. The results from these two tables demonstrate the high order of convergence of the method with respect to both space and time.

To better assess the accuracy of the introduced method, Figures 1 and 2 plot the maximum errors for different values of α with constant β and vice versa, both for u and v. These figures clearly demonstrate the exponential reduction of errors, which is a characteristic of spectral methods. Finally, in Figure 3, the graph of exact and numerical solutions is drawn together with $\alpha = 1.3$, $\beta = 1.2$ and $n_p = 14$ at T = 1, showing their good agreement.

Table 3: The L_{∞} and L_2 errors and c-orders for $\alpha = 1.5$, $\beta = 1.6$ at T = 1 with $\eta = 1/216$ (Test problem 1).

		u			v	
n_p	L_{∞} -error	L_2 error	c-order	L_{∞} error	L_2 error	c-order
2	1.69e - 01	1.69e - 01	_	6.65e - 01	6.65e - 01	_
4	2.55e - 03	3.01e - 03	6.05	1.16e - 01	2.46e - 01	2.51
6	1.59e - 04	3.07e - 04	4.00	1.01e - 02	1.75e - 02	3.52
8	1.53e - 04	3.65e - 04	0.05	7.77e - 03	1.46e - 02	0.38
10	1.52e - 04	4.56e - 04	0.004	7.71e - 03	1.82e - 02	0.01

Table 4: The L_{∞} and L_2 errors and c-orders for $\alpha=1.5,\ \beta=1.6$ at T=1 with $n_p=8$ (Test problem 1).

		u				v	
η	L_{∞} -error	L_2 error	c-order	-	L_{∞} error	L_2 error	c-order
1/4	1.84e - 02	5.04e - 02	_		3.39e - 01	6.46e - 01	_
1/16	2.52e - 03	6.34e - 03	2.86		1.00e - 01	1.89e - 01	1.76
1/64	5.34e - 04	1.29e - 03	2.24		2.58e - 02	4.89e - 02	1.94
1/256	1.29e - 04	3.07e - 04	2.05		6.57e - 03	1.23e - 02	1.97

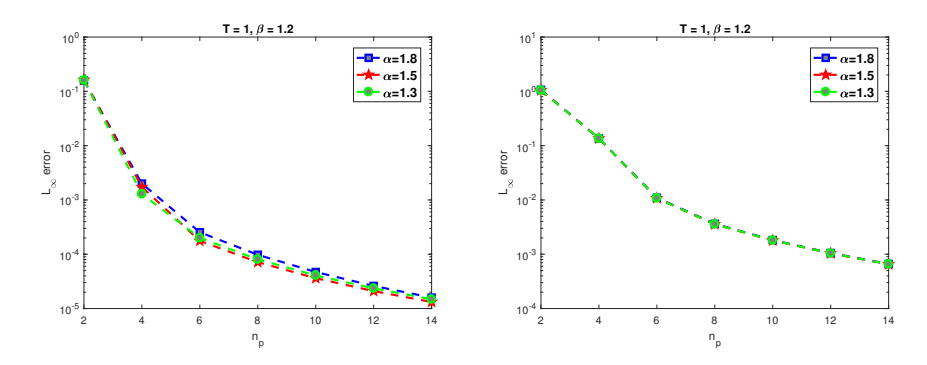


Figure 1: The L_{∞} errors of u (left) and v (right) as functions of n_p and $\eta=1/n_p^3$ for $\beta=1.2$ and different values of α at T=1 (Test problem 1).

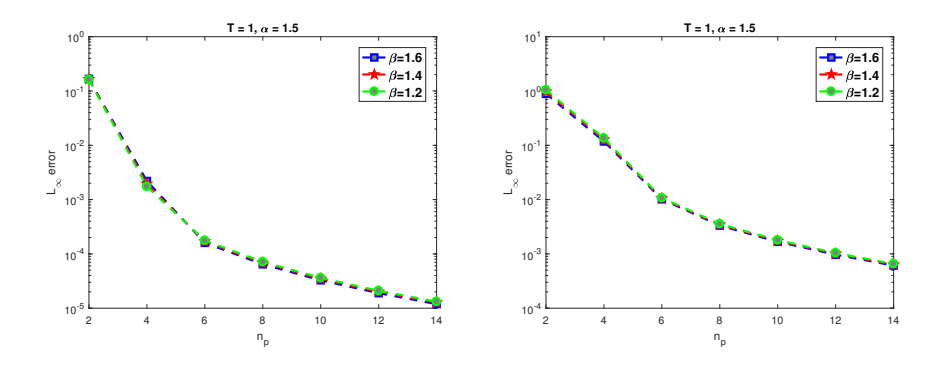


Figure 2: The L_{∞} errors of u (left) and v (right) as functions of n_p and $\eta = 1/n_p^3$ for $\alpha = 1.5$ and different values of β at T = 1 (Test problem 1).

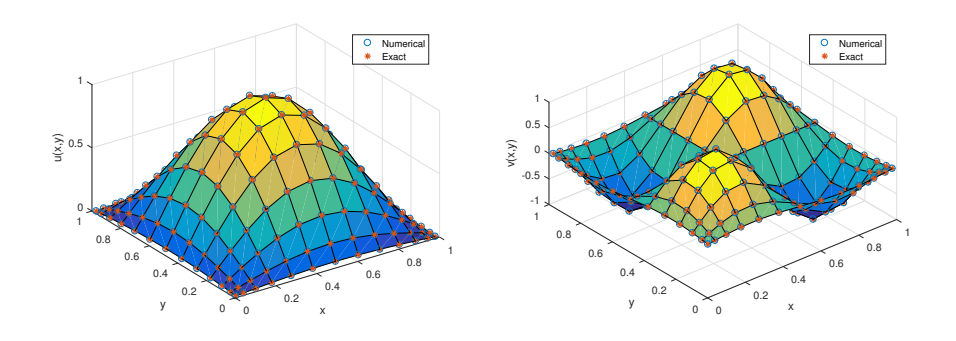


Figure 3: Surfaces for the numerical and exact solutions of u (left) and v (right) for $\alpha = 1.3$, $\beta = 1.2$ and $n_p = 14$ at T = 1 (Test problem 1).

		α =	$= 1.8, \ \beta = 1.6$	3	α =	$\alpha = 1.5, \ \beta = 1.8$				
n_p	η	L_{∞} -error	L_2 error	c-order	L_{∞} error	L_2 error	c-order	CPU-Time		
2	1/8	9.30e - 03	9.29e - 03	_	1.83e - 02	1.83e - 02	_	0.03		
4	1/64	2.03e - 02	2.05e - 02	1.12	2.57e - 02	2.62e - 02	-0.49	0.06		
6	1/216	7.06e - 04	1.51e - 03	4.85	8.62e - 04	1.66e - 03	4.90	0.34		
8	1/512	1.73e - 04	3.46e - 04	2.02	1.91e - 04	3.72e - 04	2.17	1.73		
10	1/1000	1.13e - 04	2.24e - 04	0.61	1.28e - 04	2.52e - 04	0.58	7.61		
12	1/1728	6.55e - 05	1.52e - 04	0.79	7.49e - 05	1.76e - 04	0.76	36.1		
14	1/2744	4.08e - 05	1.09e - 04	0.68	4.73e - 05	1.30e - 04	0.66	107.2		

Table 5: The L_{∞} and L_2 errors and c-orders for u at T=1 (Test problem 2).

Test problem 2

As another example, consider the nonlinear coupled KGZ equation (1) on domain $\Omega = [-1, 1]^2$ with the following exact solutions

$$u(x, y, t) = t^2 \cos(\frac{\pi}{2}x)\cos(\frac{\pi}{2}y), \quad v(x, y, t) = t^2 \cos(\frac{3\pi}{2}x)\cos(\frac{3\pi}{2}y).$$
 (38)

As before, the right-hand side functions f and g can be obtained by inserting these solutions into Equation (1) as

$$\begin{split} f(x,y,t) &= \left(\frac{\Gamma(3)t^{2-\alpha}}{\Gamma(3-\alpha)} + \frac{\pi^2}{2}t^2 + t^2 + t^4\cos(\frac{3\pi}{2}x)\cos(\frac{3\pi}{2}y)\right)\cos(\frac{\pi}{2}x)\cos(\frac{\pi}{2}y) \\ &+ t^6\left(\cos^3(\frac{\pi}{2}x)\cos^3(\frac{\pi}{2}y)\right), \\ g(x,y,t) &= \left(\frac{\Gamma(3)t^{2-\beta}}{\Gamma(3-\beta)} + \frac{9}{2}\pi^2t^2\right)\cos(\frac{3\pi}{2}x)\cos(\frac{3\pi}{2}y) \\ &+ \pi t^4\cos^2(\frac{\pi}{2}y)\left(\frac{-\pi}{2}\sin^2(\frac{\pi}{2}x) + \frac{\pi}{2}\cos^2(\frac{\pi}{2}x)\right) \\ &+ \pi t^4\cos^2(\frac{\pi}{2}x)\left(\frac{-\pi}{2}\sin^2(\frac{\pi}{2}y) + \frac{\pi}{2}\cos^2(\frac{\pi}{2}y)\right). \end{split}$$

Similar to the previous section, in Tables 5 and 6, the L_{∞} and L_2 errors are reported along with the order of numerical convergence for u and v at T=1 in two states ($\alpha=1.8$, $\beta=1.6$, and $\alpha=1.5$, $\beta=1.8$). The corresponding execution times for the relevant programs are also provided. Once again, the results demonstrate the method's good accuracy. Additionally, Figures 4 and 5 depict maximum errors for various α 's with fixed β and vice versa, both for u and v. These graphs clearly illustrate the exponential reduction of errors, a characteristic of spectral methods. Furthermore, Figure 6 displays the graph of exact and numerical solutions alongside $\alpha=1.3$, $\beta=1.2$ at T=1, highlighting their strong agreement.

		~						
		$\alpha =$	$= 1.8, \ \beta = 1.6$	3	$\alpha =$			
n_p	η	L_{∞} -error	L_2 error	c-order	L_{∞} error	L_2 error	c-order	CPU-Time
2	1/8	4.97e + 00	4.97e + 00	_	4.31e + 00	4.31e + 00	_	0.03
4	1/64	9.86e - 01	1.03e + 00	2.33	9.11e - 01	9.92e - 01	2.24	0.06
6	1/216	7.15e - 02	1.72e - 01	3.78	7.15e - 02	1.73e - 01	3.67	0.34
8	1/512	5.47e - 03	9.57e - 03	3.70	5.36e - 03	9.50e - 03	3.73	1.73
10	1/1000	9.71e - 04	1.90e - 03	2.49	9.06e - 04	1.71e - 03	2.56	7.61
12	1/1728	4.87e - 04	1.30e - 03	0.99	4.45e - 04	1.16e - 03	1.02	36.1
1.4	1/2744	3.06e - 04	9.63e - 04	0.67	2.78e - 04	8.54e - 04	0.68	107.2

Table 6: The L_{∞} and L_2 errors and c-orders for v at T=1 (Test problem 2).

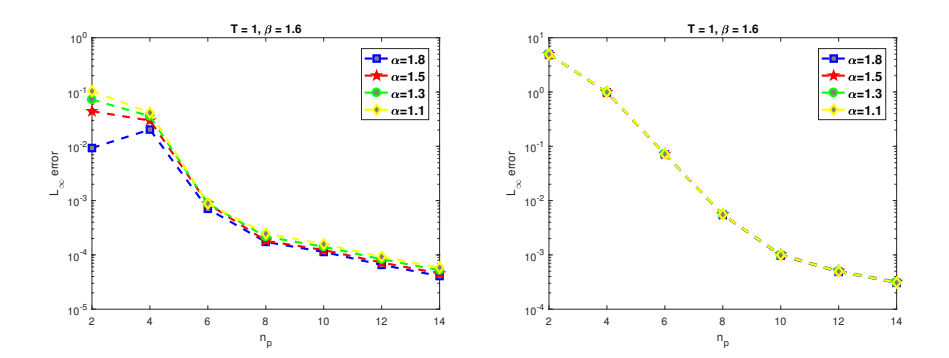


Figure 4: The L_{∞} errors of u (left) and v (right) as functions of n_p and $\eta = 1/n_p^3$ for $\beta = 1.6$ and different values of α at T = 1 (Test problem 2).

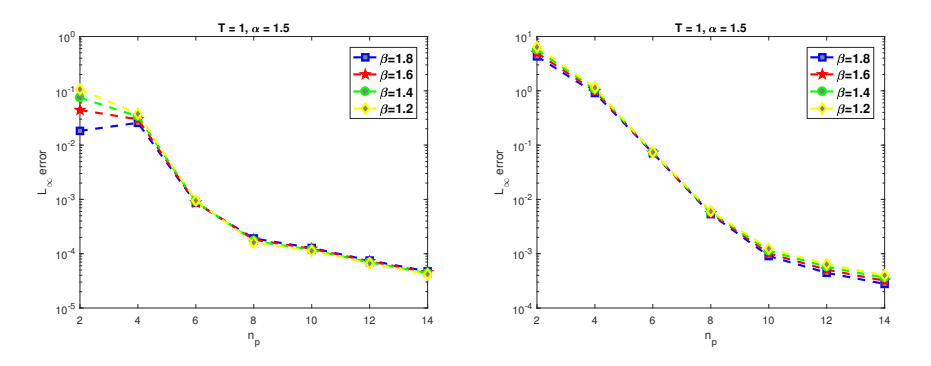


Figure 5: The L_{∞} errors of u (left) and v (right) as functions of n_p and $\eta = 1/n_p^3$ for $\alpha = 1.5$ and different values of β at T = 1 (Test problem 2).

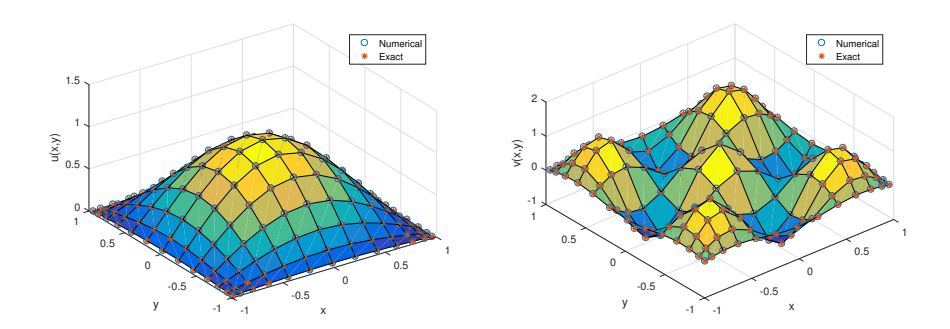


Figure 6: Surfaces for the numerical and exact solutions of u (left) and v (right) for $\alpha = 1.1$, $\beta = 1.6$ and $n_p = 14$ at T = 1 (Test problem 2).

Test problem 3

Now consider the nonlinear coupled KGZ equation (1) on $\Omega = [0,1]^2$ with exact solutions

$$u(x, y, t) = e^t \sin(\pi x) \sin(\pi y),$$

$$v(x, y, t) = e^t \sin(2\pi x) \sin(2\pi y).$$

The right-hand side functions f and g can be obtained from these solutions as

$$f(x,y,t) = (t^{2-\alpha}E_{1,3-\alpha}(t) + 2\pi^2 e^t + e^t)\sin(\pi x)\sin(\pi y) + e^{2t}\sin(\pi x)\sin(\pi y)\left(\sin(2\pi x)\sin(2\pi y) + e^t\sin^2(\pi x)\sin^2(\pi y)\right),$$

$$g(x,y,t) = (t^{2-\beta}E_{1,3-\beta}(t) + 8\pi^2 e^t)\sin(2\pi x)\sin(2\pi y) - 2\pi^2 e^{2t}\left(\cos(2\pi x)\sin^2(\pi y) + \cos(2\pi y)\sin^2(\pi x)\right).$$

where $E_{\alpha,\beta}$ is the two-parameter Mittag-Leffler function, defined as follows:

$$E_{\alpha,\beta}(z) = \sum_{k=0}^{\infty} \frac{z^k}{\Gamma(\alpha k + \beta)}, \quad (\alpha > 0, \quad \beta > 0).$$

Similar to the previous test problems, Tables 7 and 8 report the L_{∞} and L_2 errors, along with the numerical convergence order for u and v at T=1, under two parameter sets: $\alpha=1.8$, $\beta=1.2$, and $\alpha=1.5$, $\beta=1.6$. The corresponding execution times of the respective programs are also provided. Once again, the results demonstrate the method's strong accuracy.

However, in this case, due to the exponential growth of the exact solutions and the presence of the Mittag-Leffler function on the right-hand side, which involves an infinite summation and requires approximation in its computation, the resulting errors do not exhibit the exponential decay seen in the previous examples.

Table 7: The L_{∞} and L_2 errors and c-orders for u at T=1 (Test problem 3).

		$\alpha =$	$= 1.8, \ \beta = 1.2$	$\alpha =$				
n_p	η	L_{∞} -error	L_2 error	c-order	L_{∞} error	L_2 error	c-order	CPU-Time
2	1/8	2.09e - 01	2.09e - 01	_	2.11e - 01	2.11e - 01	_	0.03
4	1/64	1.10e - 02	1.40e - 02	4.24	6.12e - 02	8.07e - 02	1.78	0.06
8	1/512	4.05e - 02	1.18e - 01	1.87	1.81e - 02	5.43e - 02	1.75	1.80
10	1/1000	4.04e - 02	1.47e - 01	0.004	1.84e - 02	6.85e - 02	0.01	7.17
12	1/1728	4.03e - 02	1.76e - 01	0.002	1.85e - 02	8.26e - 02	0.007	23.4

Table 8: The L_{∞} and L_2 errors and c-orders for v at T=1 (Test problem 3).

		$\alpha = 1.8, \ \beta = 1.2$				$\alpha =$			
n_p	η	L_{∞} -error	L_2 error	c-order		L_{∞} error	L_2 error	c-order	CPU-Time
2	1/8	1.03e + 01	1.03e + 01	_		1.0144e + 01	1.0144e + 01	_	0.03
4	1/64	9.81e - 01	1.26e + 00	3.40		1.2405e + 00	1.5104e + 00	3.03	0.07
8	1/512	2.76e - 01	6.00e - 01	1.82		7.1694e - 02	1.3046e - 01	4.11	1.93
10	1/1000	2.82e - 01	7.66e - 01	0.03		6.5738e - 02	1.4958e - 01	0.12	7.71
12	1/1728	2.85e - 01	9.27e - 01	0.01		6.3338e - 02	1.7261e - 01	0.05	39.8

Additionally, Figure 7 displays the exact and numerical solutions for $\alpha = 1.3$, $\beta = 1.2$ at T = 1 at T = 1, highlighting their close agreement.

6. Conclusions

In this article, we utilized the pseudo-spectral method based on Lagrange polynomials to numerically solve the nonlinear coupled KGZ equation. The proposed method employs the finite difference technique to discretize the time variable. Additionally, we demonstrated the unconditional stability of this method. The results from three numerical examples in the previous section showcase the exponential accuracy of the method for various α 's and β 's in the interval (1,2), as presented in different tables and figures. Consequently, based on the obtained results, this method can be effectively employed to numerically solve various types of fractional differential systems.

Conflicts of Interest. The authors declare that they have no conflicts of interest regarding the publication of this article.

Acknowledgments. The authors are grateful to the anonymous reviewers for their constructive comments and helpful suggestions, which have significantly improved the quality of this manuscript.

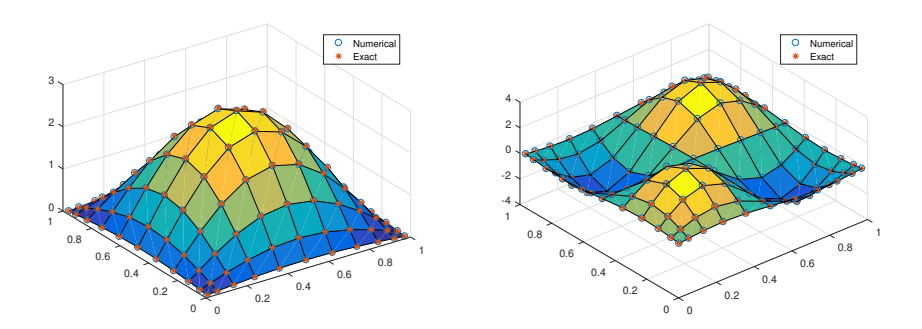


Figure 7: Surfaces for the numerical and exact solutions of u (left) and v (right) for $\alpha = 1.3$, $\beta = 1.2$ and $n_p = 12$ at T = 1 (Test problem 3).

References

- [1] D. Baleanu, J. A. T. Machado and A. C. J. Luo, Fractional dynamics and control, Springer Science & Business Media, 2011.
- [2] R. Hilfer, Applications of fractional calculus in physics, World scientific, 2000.
- [3] J. Klafter, S. C. Lim and R. Metzler, Fractional dynamics: recent advances, World Scientific, 2011.
- [4] I. Podlubny, Fractional differential equations: An introduction to fractional derivatives, fractional differential equations, to methods of their solution and some of their applications, Elsevier, 1998.
- [5] D. L. Turcotte, Fractals and chaos in geology and geophysics, Cambridge university press, 1997.
- [6] K. Diethelm, The analysis of fractional differential equations: An applicationoriented exposition using differential operators of Caputo type, Springer Berlin, Heidelberg, 2010.
- [7] F. Mainardi, Fractional calculus and waves in linear viscoelasticity: An introduction to mathematical models, World Scientific, 2010.
- [8] H. M. Baskonus, T. A. Sulaiman and H. Bulut, On the new wave behavior to the klein–gordon–zakharov equations in plasma physics, *Indian J. Phys.* **93** (2019) 393 399, https://doi.org/10.1007/s12648-018-1262-9.
- [9] M. Dehghan and A. Nikpour, The solitary wave solution of coupled klein-gordon-zakharov equations via two different numerical methods, $Comput.\ Phys.\ Commun.\ 184\ (2013)\ 2145\ -\ 2158,\ https://doi.org/10.1016/j.cpc.2013.04.010.$

- [10] T. Wang, J. Chen and L. Zhang, Conservative difference methods for the klein-gordon-zakharov equations, J. Comput. Appl. Math. 205 (2007) 430 452, https://doi.org/10.1016/j.cam.2006.05.008.
- [11] M. G. Hafez, Exact solutions to the (3+1)-dimensional coupled klein-gordon-zakharov equation using $\exp(-\phi(\xi))$ -expansion method, Alexandria Eng. J. **55** (2016) 1635 1645, https://doi.org/10.1016/j.aej.2016.02.010.
- [12] M. S. Ismail and A. Biswas, 1-soliton solution of the klein-gordon-zakharov equation with power law nonlinearity, Appl. Math. Comput. 217 (2010) 4186— 4196, https://doi.org/10.1016/j.amc.2010.10.035.
- [13] J. Li, Exact explicit travelling wave solutions for (n+1)-dimensional klein-gordon-zakharov equations, *Chaos Solitons Fractals* **34** (2007) 867 871, https://doi.org/10.1016/j.chaos.2006.03.088.
- [14] H. Triki and N. Boucerredj, Soliton solutions of the klein-gordon-zakharov equations with power law nonlinearity, *Appl. Math. Comput.* **227** (2014) 341—346, https://doi.org/10.1016/j.amc.2013.10.093.
- [15] S. Saha Ray and S. Sahoo, Comparison of two reliable analytical methods based on the solutions of fractional coupled klein–gordon–zakharov equations in plasma physics, *Comput. Math. Math. Phys.* **56** (2016) 1319 1335, https://doi.org/10.1134/S0965542516070162.
- [16] A. Akbulut and F. Taşcan, Application of conservation theorem and modified extended tanh-function method to (1+1)-dimensional nonlinear coupled klein-gordon-zakharov equation, Chaos Solitons Fractals 104 (2017) 33-40, https://doi.org/10.1016/j.chaos.2017.07.025.
- [17] J. Jia, H. Xu and X. Jiang, Fast evaluation for the two-dimensional nonlinear coupled time-space fractional klein-gordon-zakharov equations, Appl. Math. Lett. 118 (2021) #107148, https://doi.org/10.1016/j.aml.2021.107148.
- [18] F. B. Benli, Analysis of fractional klein-gordon-zakharov equations using efficient method, *Numer. Methods Partial Differential Equations* **38** (2022) 525 539, https://doi.org/10.1002/num.22662.
- [19] R. Thoudam, Numerical solutions of coupled klein-gordon-zakharov equations by quintic b-spline differential quadrature method, *Appl. Math. Comput.* **307** (2017) 50 61, https://doi.org/10.1016/j.amc.2017.02.049.
- [20] Z.-Z. Sun and X. Wu, A fully discrete difference scheme for a diffusion-wave system, Appl. Numer. Math. **56** (2006) 193 209, https://doi.org/10.1016/j.apnum.2005.03.003.
- [21] J. P. Boyd, Chebyshev and Fourier spectral methods, Dover Publications, Inc, New York, 2000.

- [22] R. A. Horn and C. R. Johnson, *Matrix analysis*, Cambridge university press, 1990.
- [23] A. Mohebbi, M. Abbaszadeh and M. Dehghan, High-order difference scheme for the solution of linear time fractional klein–gordon equations, Numer. Methods Partial Differential Equations 30 (2014) 1234 – 1253, https://doi.org/10.1002/num.21867.

Soheila Mirzaei Department of Mathematics, Faculty of Sciences, University of Zanjan, Zanjan, I. R. Iran e-mail: soheila.mirzaie@znu.ac.ir

Ali Shokri
Department of Mathematics,
Faculty of Sciences,
University of Zanjan,
Zanjan, I. R. Iran
e-mail: a.shokri@znu.ac.ir